Optimal design of quarter-wave plate with wideband and wide viewing angle for three-dimensional liquid crystal display

Wan Seok Kang, Byung-June Mun, Gi-Dong Lee, Joun Ho Lee, Byeong Koo Kim et al.

Citation: J. Appl. Phys. **111**, 103119 (2012); doi: 10.1063/1.4723819
View online: http://dx.doi.org/10.1063/1.4723819
View Table of Contents: http://jap.aip.org/resource/1/JAPIAU/v111/i10
Published by the American Institute of Physics.

Optimal design of quarter-wave plate with wideband and wide viewing angle for three-dimensional liquid crystal display

Wan Seok Kang,[1] Byung-June Mun,[1] Gi-Dong Lee,[1,a)] Joun Ho Lee,[2] Byeong Koo Kim,[2] Hyun Chul Choi,[2] Young Jin Lim,[3] and Seung Hee Lee[3,b)]
[1]*Development of Electronics Engineering, Dong-A University, Pusan 604-714, Korea*
[2]*Mobile Product Development Department, LG Display Co., Gumi, Gyungbuk 730-350, Korea*
[3]*Department of BIN Fusion Technology and Department of Polymer-Nano Science and Technology, Chonbuk National University, Jeonju, Jeonbuk 561-756, South Korea*

(Received 3 January 2012; accepted 29 April 2012; published online 30 May 2012)

In this paper, we propose an optical structure for a circular polarizer-containing film patterned retarder (FPR), which has wideband and wide-view properties in a stereoscopic three-dimensional (3D) display. The FPR consists of a patterned $\lambda/4$ *A*-plate, a biaxial $\lambda/2$ plate, and a positive *C*-plate. We calculate the phase retardation of each film in the entire visible wavelength with the Stokes vector and the Muller matrix method. We demonstrate the excellent 3D characteristics of the proposed polarizer in the oblique direction by comparing the calculated light leakage of the proposed optical configuration with that of the conventional configuration. We calculate that the crosstalk of the proposed configuration is reduced to 0.39% for the left image and 0.29% for the right image in the horizontal oblique direction and to 0.37% for the left image and 0.29% for the right image in the vertical oblique direction (polar angle = 70°). These results indicate that the proposed configuration improves crosstalk by approximately 90% compared to the conventional mode. © *2012 American Institute of Physics*. [http://dx.doi.org/10.1063/1.4723819]

I. INTRODUCTION

Recently, many display devices have begun to require three-dimensional (3D) effects to replace two-dimensional (2D) flat images. There are two major techniques for displaying 3D images: auto-stereoscopic and stereoscopic. For auto-stereoscopic 3D displays, the two main methods that have been developed are the lenticular lens method[1,2] and the parallax barrier method.[3] These do not require 3D glasses because the left and right images are spatially separated onto two sources of oriented light through geometric devices. However, auto-stereoscopic displays have problems such as deterioration of resolution, the 3D moiré effect, difficulty in 2D/3D switching, and a fixed viewing angle.[4] On the other hand, stereoscopic displays require 3D glasses to separate left and right images. The 3D glasses are either active retarder type[5,6] or passive retarder type using patterned retarder (PR) film with polarization.[7] The passive type with film PR (FPR) is proposed as the better selection for home applications and 3D cinemas because they are low cost, use lightweight glasses, have a simple fabrication process, are flicker free, and have wide-viewing angles. FPR retardation films used to divide the left and right images are manufactured using reactive mesogen (RM) materials. Retardation film not only has properties in the oblique direction, such as change of optical axis and phase retardation but also can cause color differences due to wavelength dispersion. Thus, the drawbacks for the FPRs are image quality deterioration and crosstalk at off-normal axis, which is the overlap of left and right images.

In this paper, we propose a novel optical configuration for the FPR stereoscopic 3D display with the desirable optical properties of wideband image quality and wide-viewing angle in the oblique direction. This configuration uses a patterned $\lambda/4$ *A*-plate for the left and right images with a plain biaxial $\lambda/2$ plate and a plain positive *C*-plate. We apply a biaxial $\lambda/2$ plate and a patterned uniaxial $\lambda/4$ *A*-plate to achieve the wideband property of the left and right images and apply a positive *C*-plate to achieve the wide viewing angle property. Based on the Stokes vector and the Muller matrix method, we calculate the phase retardation of each film and simulate the optical configuration on the Poincaré sphere over the entire visible wavelength spectrum using the TECHWIZ LCD made by SANAYI system. Specifically, we optimize the proposed configuration in the horizontal and vertical viewing angles (polar angle $\theta = 70°$, which induces maximum light leakage generally[8]), for applications to TV and notebook designs. We compare the calculated results of the proposed method to those of the conventional optical configuration to confirm optical enhancement.

II. A CONVENTIONAL OPTICAL CONFIGURATION USING THE FPR FOR 3D DISPLAY

The structure of the FPR stereoscopic 3D display uses a patterned retardation film made of RM material and normal optical films. Generally, the FPR stereoscopic display uses a circular polarizer to divide left and right images because a display that uses a linear polarizer can easily cause dizziness due to light leakage during viewer head rotation. Figure 1 shows the conventional optical configuration for the FPR LCD 3D display,[9] which consists of a polarizer and glasses, each with a $\lambda/4$ *A*-plate with ±45° direction in the left and

a)Electronic mail: gdlee@dau.ac.kr.
b)Electronic mail: lsh1@chonbuk.ac.kr.

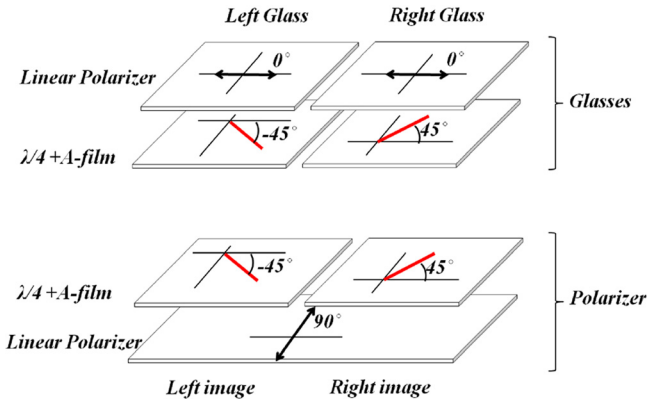

FIG. 1. Conventional configuration of the FPR structure for 3D display.

right areas, respectively. This configuration effectively blocks image crosstalk in the normal direction. However, 3D display quality is deteriorated at the oblique viewing angle due to a shift of the optical axis by the deviation angle δ and a change of the retardation value Γ in each optical film.[10] Also, dispersion of the refractive index of the optical films across the wavelengths[11,12] can affect the width of the viewing angle.

Figure 2 shows why the polarization states of light on the left and right areas are changed in the oblique direction on the Poincaré sphere. The symbols ○, □, and △ in Fig. 2 express the polarization states of the light for blue ($B = 450$ nm), green ($G = 550$ nm), and red wavelengths ($R = 630$ nm), respectively. As shown in Fig. 2(a), the start position of the conventional configuration in the normal direction is $-S_1$ when the light passes through the linear vertical polarizer. After passing through the left and right patterned $\lambda/4$ A-plates, the respective polarizations of the light rotate to the positions $L_{i(i=r,g,b)}$ and $R_{i(i=r,g,b)}$ relative to $-S_1$. The amount of rotation is equal to the retardation of the $\lambda/4$ A-plate, with centered positions S_2 and $-S_2$, the positions of the patterned $\lambda/4$ A-plates for the left and right images, respectively. Here, green wavelengths obtain excellent circular polarization states; however, blue and red wavelengths obtain elliptical polarization states due to the wavelength dispersion property.

In the oblique direction, more serious problems are encountered. Figure 2(b) shows that the position of the optical

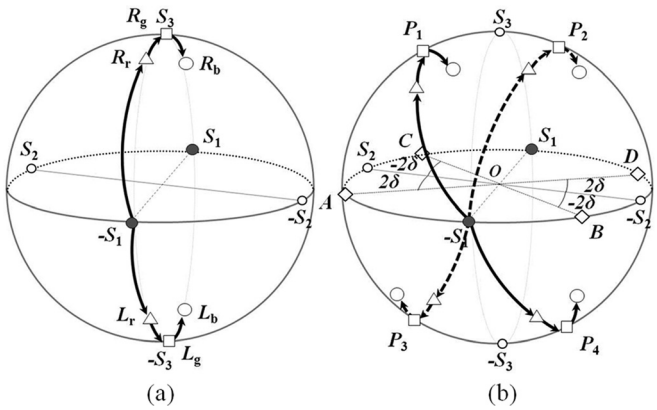

FIG. 2. Polarization state of the conventional configuration on the Poincaré sphere: (a) polarization path in the normal direction and (b) polarization path in the horizontal (linear line) and vertical (dashed line) directions. Subscripts r, g, and b represent the red, green, and blue wavelengths, respectively.

axis of the left $\lambda/4$ A-plate deviates from $-S_2$ with deviation angle δ to positions B and D, in the horizontal (linear line) and vertical (dashed line) directions, respectively. Similarly, for the right $\lambda/4$ A-plate, the optical axis deviates from S_2 with deviation angle δ to positions A and C. Furthermore, the oblique observation angle changes the retardation value of the $\lambda/4$ A-plate. Thus, the final polarization positions P_1, P_2, P_3, and P_4 considerably deviate from a circle S_1-S_3 after passing through the divided patterned $\lambda/4$ A-plates on the left and right sides due to the changes of phase retardation and optical axes in the oblique viewing angle. Therefore, the conventional optical configuration produces many residual images to the viewer due to the deficient separation of images. Thus, in order to achieve an excellent 3D image in the oblique and normal directions, these problems of degraded 3D image quality in the FPR system must be overcome.

III. A FPR SYSTEM WITH WIDE-BAND AND WIDE VIEWING CHARACTERISTICS

To completely separate the two images into left- and right-handed circular polarization states over all visible wavelengths in both normal and oblique directions, we must design a system that is wideband in the normal direction and that has a wide-viewing angle in the oblique direction. Previous studies[13,14] have demonstrated that the wideband property for circular polarization can be achieved by applying a $\lambda/2$ A-plate and a $\lambda/4$ A-plate, when the optical axes of the $\lambda/2$ A-plate ($\phi_{\lambda/2}$) and $\lambda/4$ A-plate ($\phi_{\lambda/4}$) satisfy the equation $\phi_{\lambda/4} = 2\phi_{\lambda/2} \pm 45°$, and when the optimized $\phi_{\lambda/2}$ and $\phi_{\lambda/4}$ are 15° and 75°, respectively. However, this optimized optical configuration cannot provide excellent optical characteristics in the oblique direction because the optical parameters of each birefringence layer change as described above.

In order to avoid the optical deterioration of the circular polarizer in the oblique direction, we propose the application of a biaxial film and a C-plate to the wideband circular polarizer.[15,16] Therefore, we apply a $\lambda/4$ A-plate, a biaxial $\lambda/2$ plate, and a positive C-plate to the FPR system and optimize the optical configuration of each film in order to obtain excellent 3D characteristics.

Figure 3 shows the optical structure of the FPR system using a $\lambda/2$ biaxial film in place of the $\lambda/2$ A-plate and using a positive C-plate on the patterned $\lambda/4$ A-plate. In the polarizer, the combination of the $\lambda/2$ biaxial film and the patterned $\lambda/4$ A-plate provides the wideband property, and the combination of the $\lambda/2$ biaxial film and the positive C-plate provides the wide viewing-angle property. In the eyeglasses, we apply only the uniaxial $\lambda/2$ A-plate and the $\lambda/4$ A-plate because the wide viewing property is not required in the glasses of stereoscopic 3D systems. In this paper, the optical design for the 3D display is focused on the horizontal and vertical directions because the FPR system is normally applied to large scale displays, such as TV and cinema. In the proposed FPR structure, the biaxial $\lambda/2$ film is 0.5 N_z ($N_z = (n_x - n_z)/(n_x - n_y)$). At this value, the optical axis and the retardation value are only minimally affected when the viewing angle is varied.[17] Additionally, we set the optical axis of the patterned $\lambda/4$ A-plate to 0° and 90° for the right

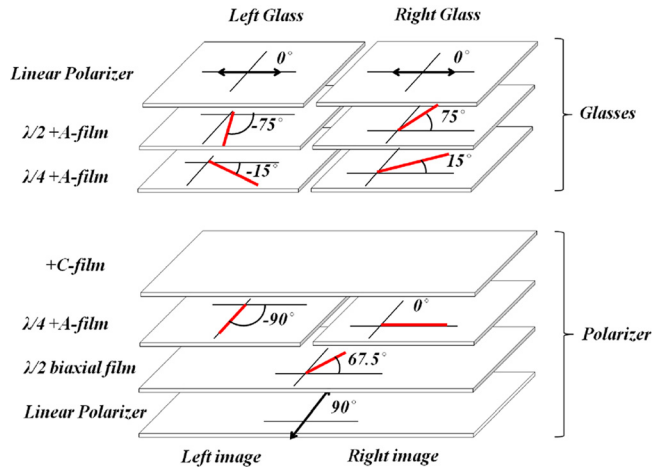

FIG. 3. The proposed configuration of the FPR structure for 3D display.

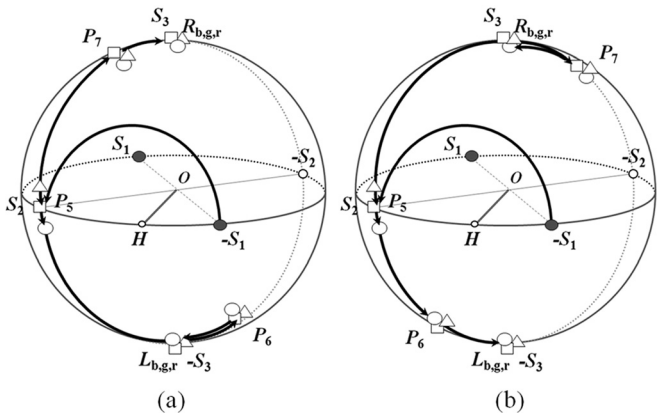

FIG. 4. Polarization states of the proposed configuration on the Poincaré sphere: (a) polarization path in the horizontal direction and (b) polarization path in the vertical direction.

and left images, respectively, because this implies that the optical axes of the patterned $\lambda/4\,A$-plate are fixed, even if the polar angle is changed in the horizontal and vertical directions. Therefore, we can simply calculate the optimized optical axis of the biaxial $\lambda/2$ film as 67.5°, satisfying the condition that $\phi_{\lambda/4} = 2\phi_{\lambda/2} \pm 45°$ to achieve the wideband property for the left and right images.

Figure 4 shows how this configuration creates circular polarization with wideband and wide viewing properties on the Poincaré sphere after light passes through the polarizer in the horizontal and vertical directions. In Fig. 4(a), H represents the position of the optical axis of the biaxial $\lambda/2$ film, which is 135° on the Poincaré sphere. In this case, the polarization states of the three wavelengths of light move to position S_2 from the start position $-S_1$ after passing through the biaxial $\lambda/2$ film with 0.5 N_z. Then, the polarization positions of the light move to opponent positions P_6 and P_7 after passing through the patterned $\lambda/4\,A$-plate of the left and right sides because the optical axes are at 90° and 0°, respectively. The retardation of the $\lambda/4\,A$-plate on the right side in the horizontal direction is smaller than the retardation in the normal direction. The retardation of the A-plate Γ_A can be calculated as follows:[18,19]

$$\Gamma_A = \frac{2\pi}{\lambda} d \left[n_e \left(1 - \frac{\sin^2\theta \sin^2\phi}{n_e^2} - \frac{\sin^2\theta \cos^2\phi}{n_o^2} \right) - n_o \left(1 - \frac{\sin^2\theta}{n_o^2} \right)^{1/2} \right], \quad (1)$$

where d represents the thickness of the film, and n_e and n_o represent extraordinary and ordinary refractive indexes of the LC material, respectively. In the case when θ is 70°, the effective retardation of the $\lambda/4\,A$-plate is 1.5708 and 1.2217 in 90° and 0° of azimuthal angle ϕ, respectively. From this, we can calculate the positions of P_6 and P_7 on the Poincaré sphere.

These positions are slightly deviated from the final goal positions S_3 and $-S_3$, which are the perfect circular polarization positions for left and right images, respectively. However, we can move the deviated polarization positions P_6 and P_7 to goal positions $-S_3$ and S_3 using a positive C-plate because the effective optical axis of the positive C-plate in the oblique horizontal direction is in the position $-S_1$. Therefore, the optimized retardation value of the positive C-plate can move the polarization states P_6 and P_7 to the circular polarization positions. We calculated the optimized retardation value of the positive C-plate using the Mueller matrix and the Stokes vector.[20,21] The four Stokes parameters can usually be written as

$$S = (S_0, S_1, S_2, S_3)^T. \quad (2)$$

The Stokes parameters for the three primary wavelengths of light that have passed through the positive C-plate can be described as follows:[22]

$$S' = R(-2\theta) \cdot M(\Gamma_C) \cdot R(2\theta) \cdot S(A+) = \begin{pmatrix} 1 & 0 & 0 & 0 \\ 0 & \cos^2 2\theta + \cos\Gamma_C \sin^2 2\theta & (1-\cos\Gamma_C)\sin 2\theta\cos 2\theta & \sin\Gamma_C \sin 2\theta \\ 0 & (1-\cos\Gamma_C)\sin 2\theta\cos 2\theta & \sin^2 2\theta + \cos\Gamma_C \cos^2 2\theta & -\sin\Gamma_C \cos 2\theta \\ 0 & \sin\Gamma_C \sin 2\theta & \sin\Gamma_C \cos 2\theta & \cos\Gamma_C \end{pmatrix} \begin{pmatrix} S_{0A+} \\ S_{1A+} \\ S_{2A+} \\ S_{3A+} \end{pmatrix} = \begin{pmatrix} S_0' \\ S_1' \\ S_2' \\ S_3' \end{pmatrix} \quad (3)$$

$$S' = (S_0', S_1', S_2', S_3')^{\mathrm{T}}, \quad S(A+) = (S_{0A+}', S_{1A+}', S_{2A+}', S_{3A+}')^{\mathrm{T}},$$

TABLE I. Calculated optimized dispersion properties of the optical anisotropy of the optical uniaxial films.

	$\Delta n/\Delta n$ (550 nm)		Δnd (nm)
	450 nm	630 nm	550 nm
Left PR film of positive *A*-plate	0.796	1.163	137.2
Right PR film of positive *A*-plate	0.831	1.128	137.2
Positive *C*-plate	0.795	1.145	74.7

TABLE II. Calculated optimized dispersion property of the optical anisotropy of the optical biaxial film.

	$\Delta n/\Delta n$ (550 nm) ($\Delta n = n_x - n_y, n_z - n_y$)		Δnd (nm) ($\Delta n = n_x - n_y$)
	450 nm	630 nm	550 nm
Biaxial film	1.0006	0.9995	272.3

where S' represents the Stokes vector of the output light, $S(A+)$ is the Stokes vector of the incident light after passing through the $\lambda/4$ patterned film, Γ_C is a retardation of the positive *C*-plate, $R(2\theta)$ and $R(-2\theta)$ are the rotating matrix and reverse rotating matrix to the principal axis, respectively, $M(\Gamma_C)$ depicts the Muller matrix for rotated polarizing components with phase retardation Γ_C, and $S(A+)$ is simply calculated by the effective retardation of the $\lambda/4$ *A*-plate. The calculated $S(A+)$ is (1, 0, −0.4282, −0.9037) and (1, 0, 0.3452, 0.9385) for the left and right image, respectively. In order to satisfy the conditions for perfect circular polarization, S' should be (1, 0, 0, ± 1). Therefore, we calculated the retardation of the positive *C*-plate such that the S_3' value of the final polarization position has a value between ± 0.998 and ± 1 according to Eq. (3). As a result, we obtained the optimized value of a positive *C*-plate which has 0.3851 rad (B), 0.3962 rad (G), and 0.3958 rad (R).

Figure 4(b) shows the improved optical parameters in the vertical direction for the polarization state of the proposed configuration. The change in the retardation value of the patterned $\lambda/4$ *A*-plate in the oblique direction is reversed in the vertical compared to the horizontal direction. However, the effective optical axis of the positive *C*-plate in the oblique vertical direction is in the position S_1, so that the polarization states P_6 and P_7 of the light passed through the patterned $\lambda/4$ *A*-plate can be moved to the circular polarization position by the positive *C*-plate.

Tables I and II show the calculated optimized retardation value of each optical film used for the *R*, *G*, and *B* wavelengths.

IV. RESULTS AND DISCUSSION

In general, the FPR method for stereoscopic 3D displays simultaneously provides the left and right images to the eyes of a viewer wearing polarization glasses. This can produce crosstalk which induces a ghost image in the oblique direction when the opposite polarized light at each lens is retransmitted after passing through the glasses. Therefore, in order to verify the optical performance of the proposed configuration, we compared the light leakage and crosstalk of the proposed configuration with that of the conventional structure that has normal $\lambda/4$ *A*-plates and FPRs with patterned wideband $\lambda/4$ *A*-plates that consist of a uniaxial $\lambda/2$ *A*-plate and a uniaxial $\lambda/4$ *A*-plate.[23] Figures 5 and 6 compare the calculated light leakage of the FPR system in the conventional, wideband, and proposed structures for the left and right images in the horizontal and vertical directions with the polar angle $\theta = 70°$. The conventional and wideband

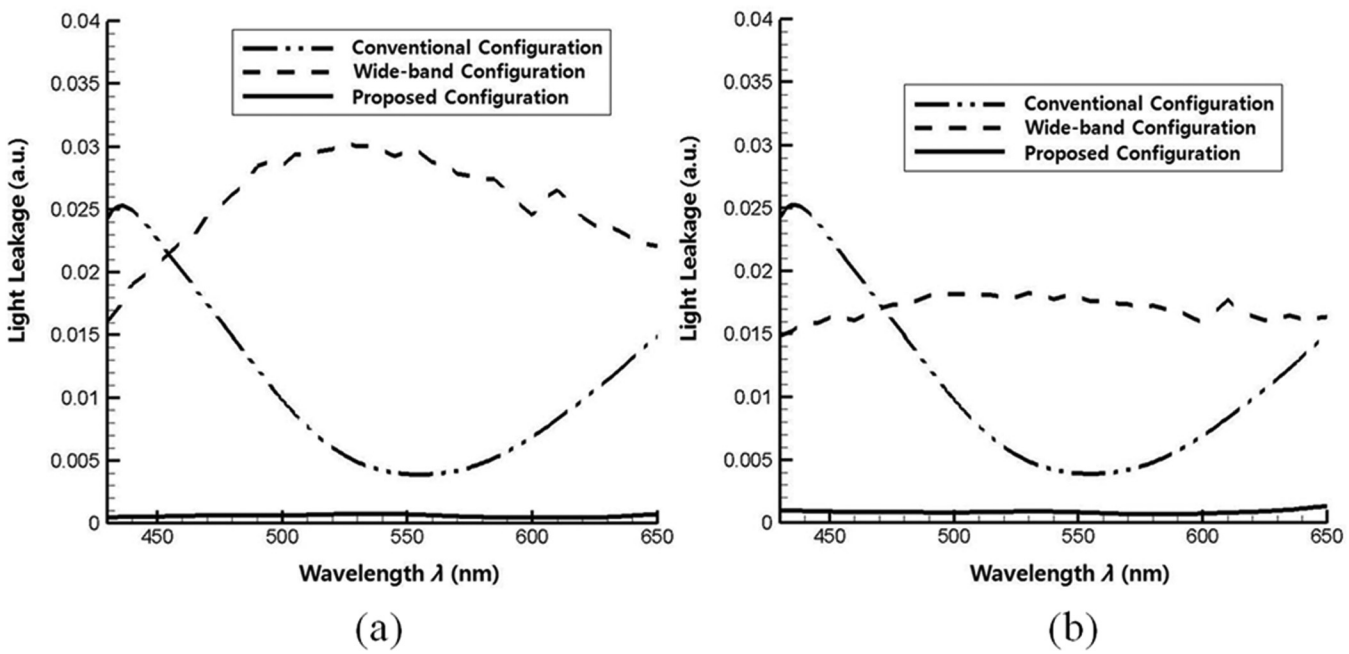

FIG. 5. Comparison of the calculated light leakage of the conventional and proposed wideband structures in the horizontal direction: (a) in the left image and (b) in the right image.

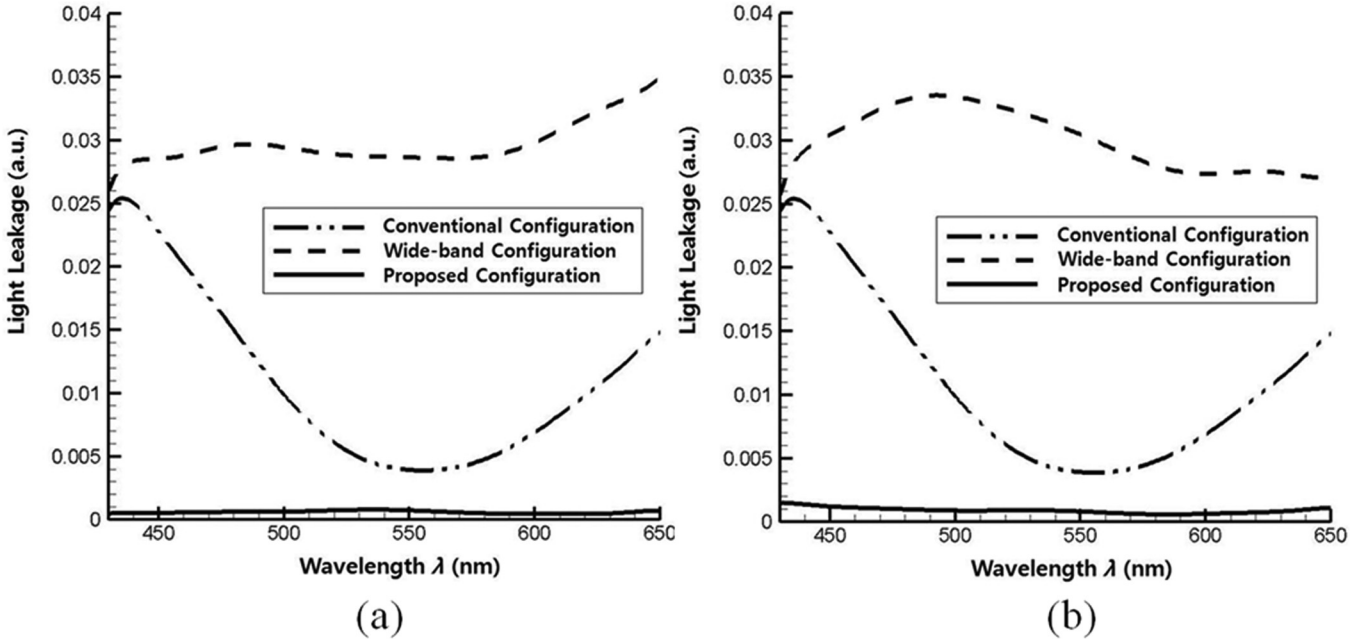

FIG. 6. Comparison of the calculated light leakage of the conventional and proposed wideband structures in the vertical direction: (a) in the left image and (b) in the right image.

FPR 3D systems experience serious light leakage in the oblique direction. However, the proposed configuration maintains an excellent dark state for the entire visible wavelength spectrum, even in the oblique direction. This indicates that final polarization states passing through the proposed structure produce a circular polarization state on the Poincaré sphere.

Figures 7 and 8 show the calculated crosstalk of the proposed configuration compared with those of the conventional and wideband configurations, in the horizontal and vertical directions. The crosstalk value can be defined as[24]

$$3D\ Crosstalk_{Left(Right)} = \frac{R(L)\_dark}{L(R)\_bright} \times 100[\%]. \quad (4)$$

Here, *L(R)_bright* is the luminance of the left and right eyes at the bright states, and *R(L)_dark* is the luminance of the left and right eyes at the dark states. The proposed optical configuration reduces crosstalk to 0.39% for the left image and 0.29% for the right image in the horizontal oblique direction, as shown in Figs. 7(a) and 7(b), and to 0.37% for the left image and 0.29% for the right image in the vertical oblique direction, as shown in Figs. 8(a) and 8(b).

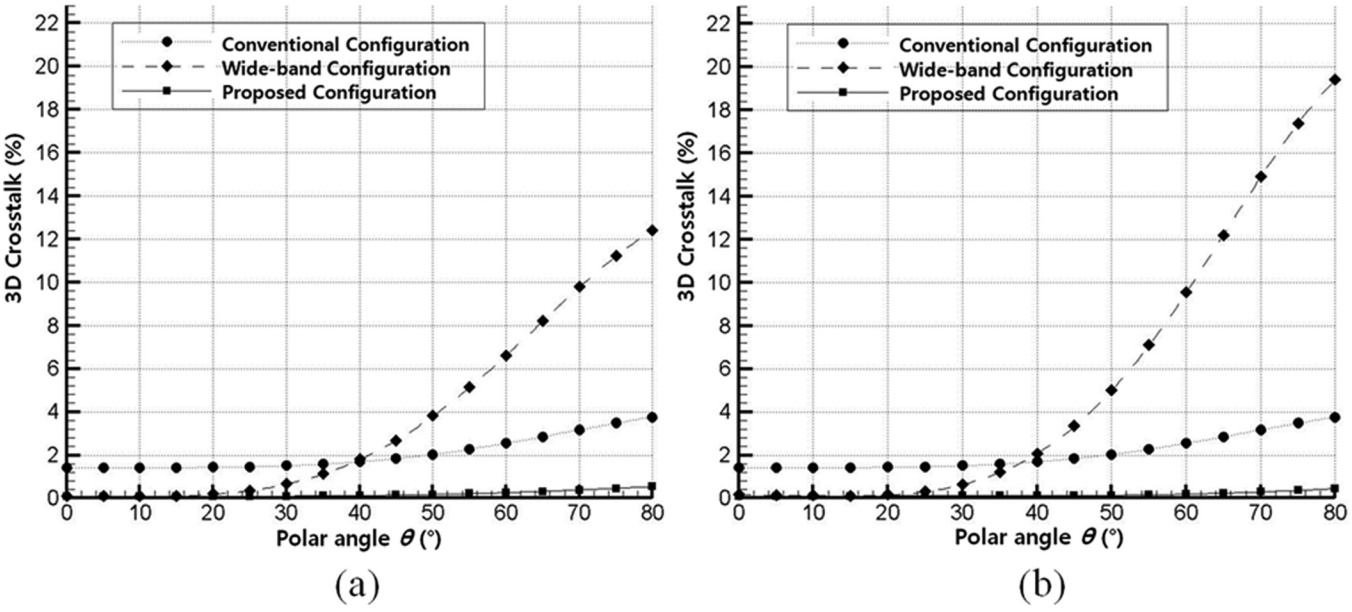

FIG. 7. Comparison of the calculated 3D crosstalk of the conventional and proposed wideband structures in the horizon direction: (a) in the left image and (b) in the right image.

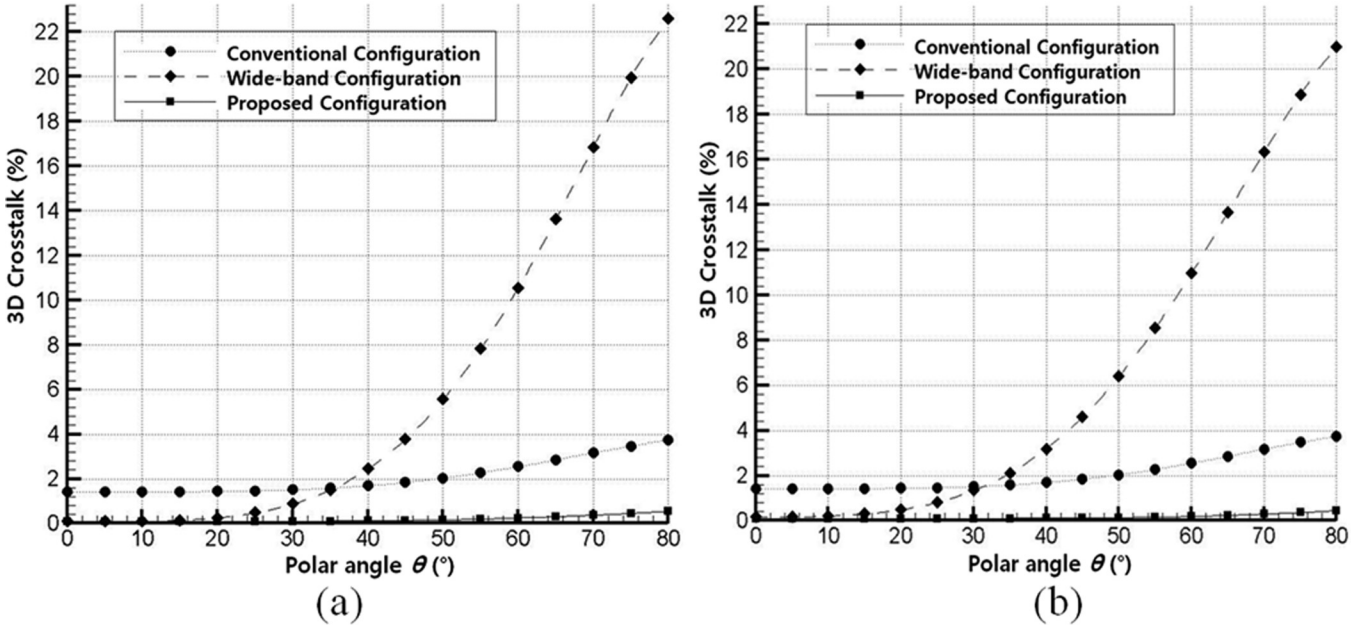

FIG. 8. Comparison of the calculated 3D crosstalk of the conventional and proposed wideband structures in the vertical direction: (a) in the left image and (b) in the right image.

V. CONCLUSION

In this study, we proposed an optical configuration of the FPR structure with a wideband and a wide viewing angle using a biaxial $\lambda/2$ film, a patterned $\lambda/4$ A-plate, and a positive C-plate. We calculated the optimized optical parameters of each film using the Mueller matrix and the Stokes vector. From this, we confirmed that the proposed FPR structure effectively reduces crosstalk in the 3D display in the oblique direction. We believe that the proposed optical configuration can be applied to stereoscopic 3D displays, which require outstanding 3D image quality and wide viewing angle.

ACKNOWLEDGMENTS

This work was supported by LG Display and World Class University program (R31-20029) funded by the Ministry of Education, Science and Technology.

[1]J. Yan, S. T. Kowel, H. J. Cho, and C. H. Ahn, Opt. Lett. **26**, 1075 (2001).
[2]C. van Berkel and J. Clarke, Proc. SPIE **3012**, 179 (1997).
[3]Y.-H. Tao, Q.-H. Wang, J. Gu, W.-X. Zhao, and D.-H. Li, Opt. Lett. **34**, 3220 (2009).
[4]G. Hamagishi, K. Taira, K. Izumi, S. Uehara, T. Nomura, K. Mashtani, A. Miyazawa, K. Koike, A. Yuuki, T. Horikoshi, Y. Yoshihara, Y. Hisatake, H. Ujike, and Y. Nakano, *Proceeding of the 15th International Display Workshop* (Society for Information Display, Niigata, Japan, 2008), p. 1099.
[5]C.-H. Tsai, W.-L. Chen, and W.-L. Hsu, SID Symp. Dig. **39**, 456 (2008).
[6]D. Suzuki, T. Fukami, E. Higano, N. Kubota, T. Higano, S. Kawaguchi, Y. Nishimoto, K. Nishiyama, and K. Nakao, SID Symp. Dig. **40**, 428 (2009).
[7]J. H. Oh, W. H. Park, B. S. Oh, D. H. Kang, H. J. Kim, S. M. Hong, J. H. Hur, and J. Jang, SID Symp. Dig. **39**, 444 (2008).
[8]J.-H. Lee, H. Choi, S. H. Lee, J. C. Kim, and G.-D. Lee, Appl. Opt. **45**, 7279 (2006).
[9]Y.-J. Wu, Y.-S. Jeng, P.-C. Yeh, C.-J. Hu, and W.-M. Huang, SID Symp. Dig. **39**, 260 (2008).
[10]P. Yeh and C. Gu, *Optics of Liquid Crystal Displays* (Wiley, New York, 1999), Chap. 9, p. 357.
[11]Y. Fujimura, T. Kamijo, and H. Yoshimi, Proc. SPIE **5003**, 96 (2003).
[12]J.-H. Lee, J.-H. Son, S.-W. Choi, W.-R. Lee, K.-M. Kim, J. S. Yang, J. C. Kim, H. Choi, and G.-D. Lee, J. Phys. D: Appl. Phys. **39**, 5143 (2006).
[13]T.-H. Yoon, G.-D. Lee, and J. C. Kim, Opt. Lett. **25**, 1547 (2000).
[14]G.-D. Lee, G.-H. Kim, T.-H. Yoon, and J. C. Kim, Jpn. J. Appl. Phys., Part 1 **39**, 2716 (2000).
[15]T. W. Ko, J. C. Kim, H. C. Choi, K. H. Park, S. H. Lee, K.-M. Kim, W.-R. Lee, and G.-D. Lee, Appl. Phys. Lett. **91**, 053506 (2007).
[16]J.-W. Moon, W.-S. Kang, H. Y. Han, S. M. Kim, S. H. Lee, Y. G. Jang, C. H. Lee, and G.-D. Lee, Appl. Opt. **49**, 3875 (2010).
[17]S.-H. Ji, J.-M. Choi, and G.-D. Lee, *Proceeding of the 15th International Display Workshop* (Society for Information Display, Niigata, Japan, 2008), p. 395.
[18]D.-K. Yang and S.-T. Wu, *Fundamentals of Liquid Crystal Devices* (Wiley, Chichester, UK, 2006), Chap. 8.3.5, p. 210.
[19]X. Zhu, Z. Ge, and S.-T. Wu, J. Disp. Technol. **2**, 2 (2006).
[20]J. E. Bigelow and R. A. Kashnow, Appl. Opt. **16**, 2090 (1977).
[21]K. Vermeirsch, A. D. Meyere, J. Fornier, and H. D. Vleeschouwer, Appl. Opt. **38**, 2775 (1999).
[22]D. Goldstein, *Polarized Light* (Dekker, 2003), Chap. 5.4, p. 75.
[23]Z. Ge, M. Jiao, R. Lu, T. X. Wu, S.-T. Wu, W.-Y. Li, and C.-K. Wei, J. Disp. Technol. **4**, 129 (2008).
[24]P.-C. Yeh, C.-W. Chen, C.-I. Huang, Y.-J. Wu, C.-H. Shih, and W.-M. Huang, SID Symp. Dig. **40**, 1431 (2009).